Effects of dark matter self-interaction on the evolution of the Sagittarius stream

Connor Hainje
Advised by Professor Mariangela Lisanti

May 2021

Abstract

asdf

Contents

1 Lambda-CDM **2**
- 1.1 Evidence for dark matter . . . 2
- 1.2 Lambda-CDM . . . 3
- 1.3 Structure formation . . . 5
- 1.4 Small-scale problems . . . 7

2 Self-interacting dark matter **9**
- 2.1 Introduction . . . 9
- 2.2 Particle physics models . . . 10
  - 2.2.1 Self-coupled scalar . . . 11
  - 2.2.2 Light mediator . . . 12
  - 2.2.3 Strong interactions . . . 12
- 2.3 Analytic description with baryons . . . 14
- 2.4 Self-interaction in simulation . . . 17

3 Sagittarius **20**
- 3.1 Overview . . . 20
- 3.2 Modern models . . . 22

4 Experimental setup **26**
- 4.1 Pipeline and parameters . . . 26
- 4.2 Equilibration . . . 28

Chapter 1

Lambda-CDM

1.1 Evidence for dark matter

In 1932, Jan Oort studied the velocities of stars near the Sun, and he found that the velocities of these stars were systematically larger than expected [37]. From the velocities of stars at a given radius in a galaxy, one can measure the gravitational mass of all objects inside that radius. As such, Oort's velocity findings were really a statement about the mass of the Milky Way. In Oort's own words, these velocities implied that the amount of gravitating matter in the Milky Way must be larger than what one can estimate by simply counting stars, with the latter falling short by roughly 30-50% [55].

The next year, Fritz Zwicky studied velocity dispersions in the Coma galaxy cluster [64, 1]. From his measurements, he found that the velocity dispersions required "10 to 100 times more mass" for the cluster to remain bound than could be accounted for by luminous matter. He concluded that there must be some large source of non-luminous matter present to account for the difference, calling the non-luminous matter "dunkle Materie", or "dark matter". This is often cited as the origin of the term.

Over the next few decades, evidence continued to mount for the existence of dark matter. Rotation curves began being considered, first by Babcock in 1939 [2] and Oort in 1940 [36]. In the words of Oort, "the distribution of mass in this object [the M31 galaxy] appears to bear almost no resemblance to that of light." Studies of globular clusters in the Milky Way indicated that at least two-to-three times as much mass must lie outside the orbit of the Sun as inside [28] (todo add Kunth 1952). Studies of binary galaxies revealed large mass-to-light ratios [40, 20] (todo add van den Bergh 1961). More galaxy clusters were studied, and the trends noted by Zwicky were found to hold generally [56]. This mounting evidence largely took the form of acknowledgement of a large mass-to-light ratio; it was not widely thought that a yet unknown form of matter was responsible.

By the 1970s, however, that would change. This was in large part due to developments on a few different fronts. First, the 1960s and 70s saw new methods for measuring the masses of galaxy clusters. Both X-ray measurements and gravitational lensing first began being used in the 1960s to obtain measurements of the masses of galaxy clusters. These studies independently confirmed the large, non-luminous masses that were indicated by the previous velocity analyses. todo add a citation

Second, the cosmic microwave background was discovered in 1965 (todo add a citation), and found to be remarkably isotropic (to better than a part in 10^4). However, strictly baryonic models of the universe suggest anisotropies in the CMB on the order of $\sim 3 \times 10^{-4}$. If the Universe contained some non-baryonic matter which interacted with photons only gravitationally, however, the predicted anisotropies are revised downward, closer to 10^{-5}, consistent with observation. Dark matter seems to fit this role perfectly. Anisotropies on this scale have been observed by more recent studies, beginning with the COBE satellite in 1992 (todo add citation).

Third, data from rotation curves became quite convincing. Rubin and Ford published improved optical data from the galaxy M31, the same galaxy studied by Oort in 1940 [50]. They found that, to even farther radii than had been previously considered, the rotation curve did *not* decrease outside the optically bright region of the galaxy, an even stronger indicator of the existence of mass not accounted for by luminous matter. Similarly, Roberts and Rots [47] and Roberts and Whitehurst [48] used measurements of 21cm hydrogen emissions to draw very similar conclusions.

Lastly, 1974 saw two watershed papers by independent research groups, each concluding that galaxies have dark halos. Einasto, Kaasik, and Saar wrote “the mass of galactic coronae halos exceeds the mass of populations of known stars by one order of magnitude, as do the effective dimensions” [15]. Similarly, Ostriker, Peebles, and Yahil wrote “the very large mass-to-light ratio and the very great extent of the spiral galaxies can perhaps most plausibly be understood as due to a giant halo of faint stars” [39]. They also note that the year prior, Ostriker and Peebles had come to a similar conclusion from considerations of stability, finding the traditional disk galaxy model to be unstable without a spherical disk [38].

1.2 Lambda-CDM

Since these discoveries, it has been widely believed among astronomers and cosmologists that non-baryonic dark matter exists, that it comprises large, spherical halos around galaxies, and that it played an integral role in the formation of the structures we can see today. Evidence has become increasingly strong with improved measurements of the anisotropy in the CMB (todo cite someone), improved rotation curves for more galaxies (todo cite someone), and better X-ray and gravitational lensing measurements.

Another major question of the twentieth century which came to be largely settled toward its end was that of the cosmological constant, Λ. This constant was introduced by Einstein into his theory of general relativity (todo explain why). Physically, this constant can be interpreted as the vacuum energy density of empty space. It is often called "dark energy" for this reason [51]. In the late 1990s, measurements of Type Ia supernovae strongly constrained Λ to be positive, giving empty space a significant, constant vacuum energy [46, 41].

These findings, combined with large amounts of evidence for the Big Bang hypothesis, are all most simply described by the ΛCDM model, sometimes called the standard model of cosmology or the concordance model [13]. The model describes the Universe as consisting of three components—the cosmological constant Λ, cold dark matter (CDM), and standard matter—operating under general relativity and coming from an origination event roughly 14 Gyr ago (the Big Bang). This rather simple model is remarkably successful at explaining the Universe.

Through its inclusion of the Big Bang event, the ΛCDM model gives an explanation for the origin of the CMB. In this model, the CMB is a residual radiation left-over from a period shortly after the Big Bang, where the Universe was hot ($>$10,000 K). As the Universe cooled and structures began to form, the photons from this period began to propagate freely in all directions.

The ΛCDM model also provides a well-tested account of the formation of structures in the Universe [13]. In the early Universe, small gravitational perturbations caused matter to collapse into small structures. These small structures—effectively just perturbations in the mass density of the Universe—created gravitational potential wells, attracting other small structures and assembling together to produce larger ones. This works especially well for describing the distribution of dark matter in the Universe, as small pockets of dark matter converge to form subhalos, halos, and larger. The case for baryonic matter and galaxy formation is more complicated, involving baryonic processes, gas dynamics, and more, but is also well-explained in the régime of hierarchical structure formation. Simulations of hierarchical structure formation have found that it is able to account well for the observed distribution of structures on the scales of galaxies, galaxy clusters, and larger. The implications of this model of structure formation are considered in more detail in the next section.

In fact, the success of this theory of structure formation serves as reason to believe that dark matter is cold (hence the "C" in ΛCDM). Dark matter being "cold" means that it was non-relativistic at the time of decoupling (the period in the early Universe when matter began to fall out of thermal equilibrium) [32]. By contrast, "hot" dark matter (HDM) would have been relativistic at the time of decoupling. Given these higher velocities, the velocity dispersion of HDM would have been non-negligible (differing from the negligible velocity dispersion of CDM). A finite velocity dispersion, however, would have prevented the dark matter particles from being bound to shallow gravitational potential wells, further preventing the formation of small-scale structures [51]. Thus, HDM fails to form structure.

On its own, ΛCDM is remarkably able to explain most of our observations of the Universe. However, there are a few cosmological problems which have arisen. One is known as the horizon problem [4, 51], which points out the the CMB is, to a high degree, isotropic, indicating that the photons making up this radiation are roughly in thermal equilibrium across the sky. However, this means that regions of the sky which are too far separated to be causally connected have remained in equilibrium. This is not explained by ΛCDM.

Another problem is the flatness problem, which points out that there is potentially a fine-tuning problem with the vanilla ΛCDM model [4, 51]. The Universe as we observe it is approximately flat today, meaning that its curvature is approximately unity. If the curvature were not unity, its deviation from flatness is expected to grow with time. As such, if the Universe is not flat, it must have been *very* close to unity at early times, meaning that this parameter may need to be "fine-tuned" to achieve a reasonable explanation. The problem is that our model should be able to describe parameters like these *without* fine-tuning.

Combining the ΛCDM model with the theory of cosmic inflation, however, solves both of these problems [4]. Inflation posits that the Big Bang was followed by a period of rapid (exponential!) inflationary expansion. Such a phenomenon would solve the horizon problem, as the whole observable Universe would have originated from a much smaller, thermally-connected region before inflation. It also solves the flatness problem, as inflation would have significantly stretched and flattened any curvature in the Universe, providing a natural explanation for the observed flatness today. In fact, this creates a sort of inverse fine-tuning problem: in this theory, any curvature which is *far* from unity requires fine-tuning.

1.3 Structure formation

As stated above, the ΛCDM model predicts structures to form in the Universe as a result of gravitational perturbations at early times. As expansion slows, the pockets of matter created by these perturbations host small gravitational potential wells, causing nearby matter to collapse inward and the growth of structure to occur. With the majority of matter in the Universe being dark matter, the first structures which occur are pockets of dark matter halos. The halos observable today are the result of the hierarchical combination of smaller halos.

The abundance of these halos can be described by extended Press-Schechter (EPS) theory [6]. This theory is grounded on rather simple assumptions: that one can use a spherical collapse model and that one can extrapolate from linear perturbation theory even into non-linear regimes. Despite these assumptions, it has been shown to give predictions about the mass spectrum of dark matter halos which are in accord with high-resolution numerical simulations.

The halos themselves can be described as virialized objects with mass

$$M_{\mathrm{vir}} = \frac{4\pi}{3} R_{\mathrm{vir}}^3 \Delta_c \rho_c, \tag{1.1}$$

where R_{vir} is the virial radius, ρ_c is the critical density of the Universe, and Δ_c is the over-density parameter. In this work, we choose to set $\Delta_c = 200$ and thus mark the virial mass and radius as with a subscript 200 instead of "vir".

The ΛCDM model also provides predictions about the internal structure of these dark matter halos. Dark matter-only N-body simulations were performed as early as 1988 [18], with higher-resolution simulations like [14] and [35] following shortly thereafter. The resulting halos from these simulations were found to agree remarkably well with a *two-power* density profile [5]

$$\rho(r) = \frac{\rho_0}{(r/a)^{\alpha}(1 + r/a)^{\beta-\alpha}}, \tag{1.2}$$

where ρ_0 is a characteristic density for the halo and a is the length scale. Special cases of this model include $(\alpha, \beta) = (1, 4)$, the Hernquist model [19], and $(\alpha, \beta) = (1, 3)$, the NFW model [35, 34]. In general, the NFW model enjoys the most usage as one of the most simple and accurate models of the mass density distribution of smaller halos.

todo Include some figures

todo Maybe include a more complete derivation of enclosed mass, NFW virial mass, hernquist total mass, etc.

The required parameters above, ρ_0 and a, are typically reformulated for the NFW distribution. In particular, we can take a given virial mass M_{200}, determine the corresponding virial radius R_{200}, and define the halo concentration $c = R_{200}/a$. The characteristic density can be found by integrating the density profile up to R_{200} and setting it equal to M_{200}. In this way, the virial mass and concentration are enough to completely specify the NFW distribution. The result is given by

$$\rho_0 = \frac{M_{200}}{4\pi a^3 f(c)}, \quad f(c) = \log(1 + c) - c/(1 + c). \tag{1.3}$$

As these halos are formed hierarchically from smaller halos, however, it has been found that the dense centers of the subhalos are able to survive the merging process. A direct result of this finding is that dark matter halos today should be full of substructure with satellite subhalos of varying sizes. In fact, simulations have shown that the number of subhalos within a halo is approximately self-similar for host halo mass [6]. While it is difficult to determine a method for identifying and counting these subhalos, it does yield a testable prediction of the small-scale structure of dark matter in the ΛCDM paradigm.

todo Discuss galaxy formation with an eye for how this leads to the missing satellites and too-big-to-fail problems

1.4 Small-scale problems

The theory of structure formation that follows from ΛCDM leads us to a few important results. First, we expect the density distributions of dark matter halos to approximately follow the NFW model, specifically with r^{-1} dependence for small r. Second, we expect rich substructure in massive dark matter halos with predictions for the number of subhalos of varying masses contained within. Third, through galaxy formation and the method of abundance matching, we obtain predictions about the number and masses of satellite galaxies that should be hosted in galaxies like the Milky Way. These three key deductions form the basis for the three classic **small-scale problems** in the ΛCDM model.

The first problem we will discuss is known as the **core-cusp problem**, which is primarily related to the first deduction above. Dark matter-only simulations of CDM halos show that the expected distribution of mass follows a density distribution that is very dense and *cuspy*, i.e. one that goes like r^{-1} at small radii (Bullock and Boylan-Kolchin 2017). As early as 1993, however, it was pointed out that such a distribution is inconsistent with observational data. In particular, "[cuspy] density profiles are excluded by gravitational lensing analyses on cluster scales and by the rotation curves of gas-rich, halo-dominated dwarf spirals on small scales" [17]. It was also recognized by Navarro, Frenk, and White, who wrote "CDM halos are too concentrated to be consistent with the halo parameters inferred for dwarf irregulars" [35].

The second problem is the **missing satellites** problem. CDM simulations predict that galaxies as large as the Milky Way should have as many as $\sim 1_000$ dark subhalos large enough to host dwarf galaxies [6]. However, as of 2019, less than 60 dwarf galaxies are known within the Milky Way [52].

There exists a potential solution to the missing satellites problem, however, in the form of abundance matching. First, one can expect that dark matter halos become less efficient at making galaxies with decreasing mass, and therefore there exists some threshold mass below which these halos remain completely dark. Then, abundance matching allows one to "solve" the missing satellites problem for the subhalos above this threshold [6].

This solution to the missing satellites problem thus makes a testable prediction. The central masses of Milky Way satellites should be consistent with the central masses of the most massive subhalos in ΛCDM simulation [6]. First probed by Boylan-Kolchin et al. in 2011 (todo cite), however, this does not hold; the most massive subhalos predicted in simulation are significantly more massive than the most massive satellite galaxies. If these subhalos do exist but have just remained dark, then we have a new problem: why did these subhalos fail to form galaxies? This is known as the **too-big-to-fail problem**, as these subhalos ought to be too big to fail to form observable galaxies. If these massive dark subhalos just do not exist, then this is a fundamental failing of the ΛCDM model's predictions in line with the missing satellites problem.

Some believe that these small-scale problems are the result of the omission of baryonic effects in ΛCDM simulations. As described above, the majority of the conflicting predictions come as the result of dark matter-only simulations. Further, in recent years, it has been shown that all of the above problems (and other small-scale issues) can be reduced or eliminated by the inclusion of stellar feedback and other effects. For example, [43] show that supernova feedback can alleviate the core-cusp problem, and [8] show that stellar feedback can explain the too-big-to-fail problem.

However, prior to these findings, researchers sought modifications to the model that would preserve the successes of ΛCDM on large scales *and* solve the small-scale problems. Some researchers have sought modifications to the model of gravity, but a more popular avenue has been the modification of the dark matter model. While it seems that integration of more sophisticated baryonic processes may be sufficient to solve the small-scale problems, there is no evidence yet that other proposed dark matter models are incorrect descriptions of the particle nature of dark matter. As such, further tests of ΛCDM and these alternative dark matter models are necessary as probes of dark matter particle physics. The alternative dark matter model that we consider in this work is *self-interacting dark matter*, or SIDM.

Chapter 2

Self-interacting dark matter

2.1 Introduction

Self-interacting dark matter (SIDM) was introduced in 2000 by Spergel and Steinhardt [53]. The model was proposed as a solution to the core-cusp and missing satellites problems, as the addition of self-interactions was thought to have three primary effects on the distribution of dark matter.

1. Self-interactions in regions of high density would cause dark matter particles to be unbound, reducing the density of halos primarily in their center region. This would yield a cored density profile rather than a cuspy one, solving the core-cusp problem.

2. It is also expected that interactions would yield a more isotropic velocity dispersion than seen in CDM as well as erase the typical triaxial ellipticity seen in halo shapes. In other words, SIDM halos should be more spherical, a testable prediction.

3. Through the processes of isotropizing the velocity dispersion and reducing density in core regions, it was also expected that substructure would be greatly reduced, lowering the number of dwarf galaxies and thereby solving the missing satellites problem. However, since the dark matter scattering rate would be naturally dependent on the dark matter density, these effects would only be expected in higher density regions. Toward the outermost radii of halos and on larger scales, the effects of self-interaction would be negligible, preserving the large-scale successes of the ΛCDM model.

One other feature of the model is that the dark matter scattering rate is naturally dependent on the dark matter density.

Shortly thereafter began a wave of numerical simulations to test these predictions. The results of these simulations were mixed. Some were focused on the evolution of galaxies and found confirmation of the predicted effects (more strongly spherical shape, cored density profile) like [7, 10]. Other simulations, like cluster and cosmological simulations, seemed to show that SIDM would be inconsistent with observation [33, 61, 62].

At the same time, constraints on the allowed self-interaction cross section began being compiled, primarily from clusters. Given the lack of knowledge of the mass of dark matter particles, cross section values are generally given as cross section-to-mass ratios, denoted σ/m. We will use the term cross section interchangeably with this. [30] used cluster simulations to limit the allowable cross section to $<$ 0.1 cm^2/g. Similarly, gravitational lensing data from the MS 2137-23 cluster was used by [31] to limit the cross section to $< 10^{-25.5}$ cm^2/GeV, approximately 0.02 cm^2/g. These cross sections were far too small to solve the small-scale problems in galaxies, as simulations like [10] suggested the necessary cross section to be in the range 10^{-25} to 10^{-23} cm^2/MeV (0.05 to 5 cm^2/g).

However, more recent simulations with higher resolution, better statistics, and updated algorithms for considering self-interactions have relaxed many of these constraints significantly, improving the viability of the model and once again sparking interest in self-interactions. Examples include [49, 42, 63, 16]. These newer, better simulations revised the previous constraints and generally show that cross sections on the order of $\sigma/m \sim 0.1$ to 10 cm^2/g are viable and consistent with observation. Of particular relevance for this thesis is [49], which put forth a novel method for computing the effects of self-interactions in N-body simulation. See Subsection 2.4 for a discussion of their method.

[57] have distilled the relevant modern observational constraints on the self-interaction cross section into a table. The data are reproduced in Table 2.1. In particular, notice that the data are consistent with a decaying cross section as the velocity scale increases. Specifically, all data (spiral galaxies and both applications of the too-big-to-fail problem) indicate that the small-scale cross-section ought to be $\gtrsim 0.5$ to 1 cm$^2/g$, but the larger-scale cross section ought to be ~ 0.1 cm^2/g or smaller. This rules out any particle models we find with a velocity-independent cross section.

todo add one of those plots that shows it changing slowly for galactic scales

todo add a discussion of what different kinds of astrophysical observations might mean different things about the particle physics properties

2.2 Particle physics models

Given that very little is known conclusively about the particle physics nature of dark matter, the introduction of the possibility of self-interactions makes way for a wealth of rich new theories. We will cover a few of the most popularly

	σ/m (cm^2/g)	$v_{\rm rel}$ (km/s)	Observation
Cores in spiral galaxies	$\gtrsim 1$	30-200	Rotation curves
TBTF in Milky Way	$\gtrsim 0.6$	50	Stellar dispersion
TBTF in Local Group	$\gtrsim 0.5$	50	Stellar dispersion
Cores in clusters	~ 0.1	1500	Stellar dispersion, lensing
Halo shape/ellipticity	$\lesssim 1$	1300	Cluster lensing surveys
Substructure mergers	$\lesssim 2$	500-4000	DM-galaxy offset
Merging clusters	$\lesssim$ few	2000-4000	Post-merger halo survival

Table 2.1: Observational constraints on the self-interaction cross section of dark matter. All listed observations are derived from sets of multiple systems. "TBTF" is the abbreviation for "too-big-to-fail." This is an abridged reproduction of the table compiled by [57]. A distinction is made between "positive observations" (above the horizontal rule) and "constraints" (below the horizontal rule) by the original authors. References to the original papers are given therein.

considered models below.

2.2.1 Self-coupled scalar

The first particle model that we consider is the simplest: a scalar particle, φ, that interacts with itself through a two-to-two coupling. This can be described by the Lagrangian

$$\mathcal{L}_{\rm int} = -\frac{\lambda}{4!}\varphi^4. \tag{2.1}$$

From the Lagrangian, we can read off the Feynman rule for a four-point intersection to have the matrix element $i\mathcal{M} = -i\lambda$, yielding the two-to-two self-interaction differential cross-section

$$\frac{d\sigma}{d\Omega} = \frac{\lambda^2}{64\pi^2(4m^2)}. \tag{2.2}$$

Integrating over the solid angle and dividing by two to account for identical particles gives a total cross section

$$\sigma(\varphi\varphi \to \varphi\varphi) = \frac{\lambda^2}{128\pi m^2}. \tag{2.3}$$

One can easily see that this cross section does not admit any kind of velocity independence. Thus, one could make this model consistent for a small subset of scales (e.g. $\sigma/m \sim 1$ cm^2/g for dwarf galaxy scales), but then it would necessarily fail on other scales. This makes the model viable only for analyses of limited scales where the cross-section is not expected to vary greatly, but it is generally infeasible as a solution to the small-scale problems.

2.2.2 Light mediator

Perhaps the simplest model with a theory rich enough to solve all of the observed problems is one wherein dark matter self-interactions are mediated by a light particle. We will consider a model where dark matter is represented by χ and has mass m_χ, and the mediator field is ϕ with mass m_ϕ. This theory works with both scalar and vector mediators, depending on what specific theory one wants to consider. Perhaps the best motivated origin for such a model is one where the dark matter particle is charged under a spontaneously broken $U(1)$ symmetry and the mediator arises as the corresponding gauge boson [57].

Such a model would have an interaction Lagrangian given by

$$\mathcal{L}_{\text{int}} = \begin{cases} g_\chi \overline{\chi} \gamma^\mu \chi \phi_\mu & \text{(vector mediator)}, \\ g_\chi \overline{\chi} \chi & \text{(scalar mediator)}, \end{cases} \tag{2.4}$$

where we let the coupling constant be g_χ. In the non-relativistic limit, the interaction is well-approximated by the Yukawa potential [58, 59]

$$V(r) = \pm \frac{\alpha_\chi}{r} e^{-m_\phi r}, \tag{2.5}$$

where $\alpha_\chi \equiv g_\chi^2/4\pi$ is the dark fine structure constant. The $\pm$ will be set depending on whether the interaction is attractive or repulsive. For a scalar ϕ, the potential is attractive and the sign is $(-)$. For vector ϕ, the potential is attractive $(+)$ for $\chi\overline{\chi}$ scattering and repulsive $(-)$ for $\chi\chi$ and $\overline{\chi\chi}$ scattering.

Using the Yukawa potential, we can obtain the Born differential cross section in the limit that $\alpha_\chi m_\chi / m_\phi \ll 1$ to be [57]

$$\frac{d\sigma}{d\Omega} = \frac{\alpha_\chi^2 m_\chi^2}{\left[m_\chi^2 v_{\text{rel}}^2 (1 - \cos\theta)/2 + m_\phi^2 \right]^2} \tag{2.6}$$

An important implication of this formula is that the mediator mass must be positive, i.e.$m_\phi > 0$. If instead $m_\phi = 0$, we would then find that $d\sigma/d\Omega \propto v_{\text{rel}}^{-4}$, which is far too strong at small velocities to admit a solution which is consistent with observations. A small but nonzero mediator mass m_ϕ, on the other hand, allows us to "soften" this velocity-dependence to admit a more consistent model.

While quite simple, it has been shown in [59] that it is possible for it to simultaneously accommodate all important observations and solve the small scale problems.

2.2.3 Strong interactions

Some of the richest theories for self-interacting dark matter candidates that one can consider are non-Abelian gauge theories where the dark matter candidates arise as composite bound states. In these theories, the self-interaction manifests as a strong interaction.

The motivation for considering such a model comes from our experience with QCD and the visible sector [25]. For a dark matter model to be a good candidate, it must be stable over the lifetime of the Universe and be neutral under standard model phenomena. Further, we desire models in which the particles exhibit strong self-interactions. These are all properties exhibited by particles in the visible sector under QCD, so it makes sense to consider a similar theory to describe our dark matter candidate. However, we do not necessarily know the gauge group or particle properties of dark matter, leaving us a great freedom to vary the model significantly. Many of the resulting models thus have interesting and unique new physics, though these details are greatly model-dependent.

The primary free parameters of models of this kind are the confinement scale Λ (different from the cosmological constant), and the dark quark mass(es). In the event that our "dark QCD" contains no analogue to electromagnetic/weak interactions, meson-like bound states of the dark quarks could be stable [9]. These mesons can be classified as loosely pion-like, where $m \ll \Lambda$, or quarkonium-like, where $m \gg \Lambda$ [25]. There are several proposed models for each of these scenarios; one of the more well-known is the strongly-interacting massive particle, or SIMP, where the dark matter candidate is pion-like and many non-Abelian theories are possible.

Our non-Abelian model may instead look quite similar to visible QCD, wherein the primary stable bound states are baryonic in nature. In [25], it is noted that the advantage of such models is that "dark matter is automatically sufficiently stable, and no further ultraviolet model-building is needed." One such dark baryon model is "Stealth Dark Matter," proposed by the LSD collaboration, which is a scalar dark baryon under a confining $SU(4)$ theory. This theory is named *stealth* dark matter because it is found that the baryons are safe from direct detection, though it does predict a spectrum of lighter meson particles that would be possible to detect at colliders [25].

The third class of candidate particles that has received attention are dark glueballs. Glueballs are bound states of only gluons and are predicted to exist in QCD, but are very difficult to detect. Dark glueballs would then be bound states of dark gluons. Such a model is possible if all the dark fermions in the theory have masses significantly larger than Λ. In this case, glueballs may become stable under an accidental symmetry like baryons, allowing them to be the primary dark matter candidate.

The observables that could result from the above considerations are as diverse as the models themselves. One aspect of these models that wee have not considered is what the interactions with the standard model could look like. Some models predict the dark matter candidate to be neutral under standard model interactions, but its constituents to be charged. In such a case, the model would have a coupling to the photon, and it would be possible to directly detect the particle. We may also consider the case where our theory predicts fundamental fermions. It is plausible that these fermions would obtain at least part of their mass through a coupling to the Higgs boson, again providing a mechanism by which we could directly detect the particles. Kribs and Neil provide more details of these observables, as well as collider-specific results, in [25].

2.3 Analytic description with baryons

In 2014, Kaplinghat et al. [24] provided a semi-analytic approach to deriving equilibrium solutions for the dark matter density profile using the Jeans equation. This approach allows for the inclusion of the gravitational potential of both the dark matter and baryons, providing the means to make predictions about the effects of baryons on the dark matter distribution.

They begin with the Jeans equation, rewritten via Poisson's equation. They assume constant velocity dispersion σ_0 and that the dark matter density profile is given by $\rho(\mathbf{r}) = \rho_0 \exp(h(\mathbf{r}))$. Plugging these in yields

$$\nabla_x^2 h(\mathbf{x}) + (4\pi G r_0^2/\sigma_0^2)\left[\rho_B(\mathbf{x}) + \rho_0 \exp\left(h(\mathbf{r})\right)\right] = 0, \tag{2.7}$$

where we have introduced a length scale r_0, a dimensionless length $x = r/r_0$, and the baryonic density profile ρ_B.

As a simple test of this equation, we can consider the case where baryonic matter dominates. Then, the $\exp(h)$ term can be neglected, yielding

$$\nabla_x^2 h(\mathbf{x}) + (4\pi G r_0^2/\sigma_0^2)\rho_B(\mathbf{x}) = 0. \tag{2.8}$$

Using Poisson's equation, $4\pi G\rho(r) = \nabla_r^2 \Phi(r)$, this becomes

$$\nabla_x^2 h(\mathbf{x}) + \frac{1}{\sigma_0^2}\nabla_x^2 \Phi(\mathbf{x}) = 0. \tag{2.9}$$

Integrating over x gives the solution

$$h(\mathbf{x}) = \frac{1}{\sigma_0^2}\left(\Phi(0) - \Phi(\mathbf{x})\right), \tag{2.10}$$

which corresponds to a dark matter density of

$$\rho(\mathbf{x}) = \rho_0 \exp\left[\frac{1}{\sigma_0^2}\left(\Phi(0) - \Phi(\mathbf{x})\right)\right]. \tag{2.11}$$

The authors then recommend defining the core radius as the radius at which the density is half the initial density, $\rho_0/2$. Such a position would give $h(\mathbf{r}_c) = -\ln 2$, or

$$\Phi(0) - \Phi(\mathbf{r}_c) = -\sigma_0^2 \ln 2. \tag{2.12}$$

Thus, the core size would depend only on the baryonic potential in the case where it dominates, which follows from these assumptions but stands in marked contrast to observation, where the baryonic contribution does not dominate.

At this point, the authors make the move to consider the spherically symmetric case. To do so, they approximate the Milky Way baryon distribution, ρ_B, by a Hernquist profile whose spherical enclosed mass distribution approximates the true enclosed mass distribution. The Hernquist density profile is given by

$$\rho_B(r) = \frac{\rho_{B0}}{(r/r_0)(1+r/r_0)^3}, \tag{2.13}$$

corresponding to a gravitational potential of

$$\Phi_B(r) = -\frac{GM_B}{r+r_0}, \tag{2.14}$$

where M_B is the total mass of baryons in the Milky Way. The free parameters can be set by finding r_0 and $\Phi_B(0)$ such that the circular velocity $V_B(r_0)^2 = -\Phi_B(0)/4$ matches observation. The authors give $\sqrt{-\Phi_B(0)} = 365$ km/s and $r_0 = 2.7$ kpc to be a good fit. We can thus find the core size by solving

$$-\sigma_0^2 \ln 2 = \Phi_B(0) - \Phi_B(r_c) = \Phi_B(0)\left(1 - \frac{1}{1+r_c/r_0}\right), \tag{2.15}$$

which gives

$$r_c \approx \frac{r_0\sigma_0^2 \ln 2}{-\Phi_B(0)} = \frac{r_0\sigma_0^2 \ln 2}{4V_B(r_0)^2}. \tag{2.16}$$

For a typical value of σ_0, on the order of 150 km/s, we thus obtain

$$r_c \approx 0.3 \text{ kpc}\left(\frac{r_0}{2.7 \text{ kpc}}\right)\left(\frac{\sigma_0}{150 \text{ km/s}}\right)^2\left(\frac{183 \text{ km/s}}{V_B(r_0)}\right)^2, \tag{2.17}$$

which is quite small.

Let's continue under the assumption that the Milky Way is spherically symmetric and that its baryon profile can be approximated by a Hernquist profile, but drop the assumption that baryons dominate the potential. To begin, we will rewrite the Jeans equation in a spherically symmetric system. First, note that

$$\frac{4\pi G r_0^2}{\sigma_0^2}\rho_B(x) = \frac{1}{\sigma_0^2}\nabla_x^2\Phi_B(x) = \nabla_x^2\left(\frac{\Phi_B(0)}{\sigma_0^2}\frac{1}{1+x}\right). \tag{2.18}$$

Thus, we can rewrite the Jeans equation as

$$\begin{aligned} 0 &= \nabla_x^2\left(h(x) + \frac{\Phi_B(0)}{\sigma_0^2}\frac{1}{1+x}\right) + \frac{4\pi G\rho_0 r_0^2}{\sigma_0^2}e^{h(x)} && (2.19)\\ &= \frac{1}{x^2}\frac{\partial}{\partial x}\left[x^2\frac{\partial}{\partial x}\left(h(x) + \frac{\Phi_B(0)}{\sigma_0^2}\frac{1}{1+x}\right)\right] + \frac{4\pi G\rho_0 r_0^2}{\sigma_0^2}e^{h(x)}. && (2.20)\end{aligned}$$

We now introduce a new dimensionless variable, $y = x/(1+x)$. Substituting it in yields

$$\frac{(1-y)^4}{y^2}\frac{\partial}{\partial y}\left[y^2\frac{\partial}{\partial y}\left(h(y)+\frac{\Phi_B(0)}{\sigma_0^2}(1-y)\right)\right]+\frac{4\pi G\rho_0 r_0^2}{\sigma_0^2}e^{h(y)}=0. \tag{2.21}$$

Simplifying, we then obtain

$$\frac{1}{y^2}\frac{\partial}{\partial y}\left(y^2\frac{\partial h}{\partial y}\right)-\frac{2\Phi_B(0)}{\sigma_0^2}\frac{1}{y}+\frac{4\pi G\rho_0 r_0^2}{\sigma_0^2}\frac{e^{h(y)}}{(1-y)^4}=0. \tag{2.22}$$

The authors recommend that this equation be simplified by letting a_0 be the coefficient for the $\exp(h(y))$ term and $a_1 = -\Phi_B(0)/\sigma_0^2$. The boundary conditions imposed on the equation are then $h(0) = 0$ and $h'(0) = -a_1$, which enforce a core in the center.

We can then solve this equation approximately within the core by approximating the third term by a_0, equivalent to setting $y = 0$ in this term alone. The resulting equation has approximate solution

$$h(y) \approx -a_1 y - \frac{1}{6}a_0 y^2. \tag{2.23}$$

In the case that baryons dominate, $a_1 \gg a_0$ and the y^2 term becomes negligible. The core radius then is given by the solution to

$$\frac{\ln 2}{a_1} = \frac{r_c}{r_0 + r_c}, \tag{2.24}$$

which is

$$r_c = r_0\frac{\ln 2}{a_1 - \ln 2} \approx \frac{r_0\sigma_0^2\ln 2}{-\Phi_B(0)}, \tag{2.25}$$

the same result as we derived before. In the case that dark matter dominates, $a_0 \gg a_1$ and the y term becomes negligible. The core radius is given by the solution to

$$\frac{6\ln 2}{a_0} = \left(\frac{r_c}{r_0 + r_c}\right)^2, \tag{2.26}$$

which is

$$r_c = r_0\frac{\sqrt{6\ln 2}}{a_0 - \sqrt{6\ln 2}} \approx r_0\sqrt{6\ln 2/a_0} = \sqrt{\frac{3\ln 2\,\sigma_0^2}{2\pi G\rho_0}}. \tag{2.27}$$

The authors reference an SIDM simulation of a Milky Way-sized halo with a resulting inner density of approximately 2.2 GeV c^{-2} cm^{-3}. In the dark matter dominated limit, we thus estimate the core size to be approximately 5.5 kpc, which is consistent with simulation.

For the case where neither baryons nor dark matter dominate, the authors give the following result for the core size

$$r_c \approx r_0\frac{\sqrt{1+\frac{2\ln 2\,a_0}{3a_1^2}}-1}{1+\frac{a_0}{3a_1}-\sqrt{1+\frac{2\ln 2\,a_0}{3a_1^2}}}. \tag{2.28}$$

However, we have potentially a family of solutions parameterized by a_0 and a_1. As a criterion for consistent selection, then, the authors adopt the following convention. Let r_1 be the radius at which the average dark matter particle has undergone one interaction. We choose the values of a_0 and a_1 such that the mass and total energy within r_1 match the values that one would have had in the absence of self-interactions. To compare against "the absence of self-interactions," one can look at, for example, an NFW profile that approximately fits the considered galaxy.

For the Milky Way, we can consider the self-interaction cross section required for r_1 to be approximately the solar radius, 8.5 kpc. The local dark matter density is known to be approximately 0.2 GeV c^{-2} cm^{-3}. We can also estimate the age of the Milky Way to be 10 Gyr. Thus, we expect the average number of scatterings to be approximately

$$\left(0.2 \text{ GeV } c^{-2} \text{ cm}^{-3}\right)(150 \text{ km/s})\,(\sigma/m)\,(10 \text{ Gyr})\,. \tag{2.29}$$

A self-interaction cross section of about $\sigma/m = 1$ barn/GeV (0.56 cm^2/g) sets this to one scattering event per particle. As we have seen, this cross section is consistent with observations on the scales of galaxies and is capable of solving the small-scale problems.

The authors specifically consider values of σ_0, ρ_0, and r_1 that approximate the Milky Way in the case that the no-self-interaction halo is well described by an NFW profile. They find that $r_1 = 15$ kpc, $\sigma_0 = 165$ kpc, $\sigma/m = 1$ barn/GeV, and $\rho_0 = 14$ GeV c^{-2} cm^{-3} gives a good fit. When plugged into Equation 2.28, this yields an expected core size of 0.43 kpc. The resulting density profiles are shown in Figure 2.1. In particular, note that the dashed red curve (SIDM analog to the standard NFW Milky Way) attains half its central density at approximately 0.5 kpc, in line with the analytic expectation.

2.4 Self-interaction in simulation

In this work, we will be exploring the introduction of self-interaction in predictions about the infall of the Sagittarius dwarf galaxy and, specifically, the formation of its stream. This is done through the use of N-body simulations. As such, we present a description of how these self-interactions are modeled in simulation. We choose to use GIZMO [21] for our simulations, and the implementation of self-interactions therein is the one described by [49]. Much of the following discussion comes in large part from [49].

In our simulation, we consider some number of "macro-particles," each of which represents an ensemble of dark matter particles, a patch of the dark matter phase-space density. We let each macro-particle have mass m_p, and we keep this mass consistent across all dark matter macro-particles. Since we consider the macro-particle as representing a patch of the phase-space density, we consider its position to be centered at some point $\mathbf{x}$ but spread out according to a kernel

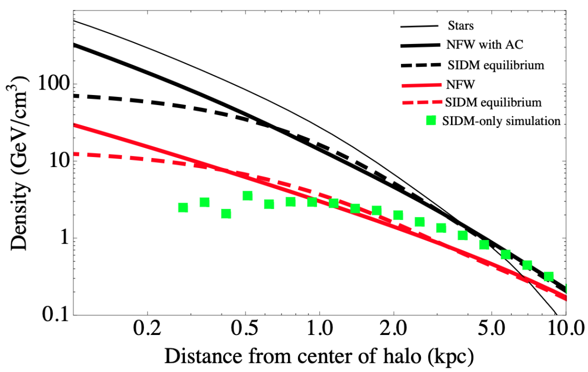

Figure 2.1: Mass density distributions for a Milky Way-sized halo. The green boxes show the result of a dark matter-only SIDM simulation. The thick solid lines show NFW distributions, both adiabatically contracted (black) and not (red). (We focus only on the non-adiabatically contracted case in this study.) The dashed lines show the corresponding analytic SIDM profiles expected from the results of the Jeans equation-based formalism. This figure is reproduced from Figure 1 of [24].

$W(r, h)$. Here, r is the distance from the center of the macro-particle and h is a smoothing length. In GADGET-2, from which GIZMO is built, the kernel is given by

$$W(r, h) = \frac{8}{\pi h^3} \begin{cases} 1 - 6(r/h)^2 + 6(r/h)^3 & 0 \le r/h \le 1/2, \\ 2(1 - r/h)^3 & 1/2 < r/h \le 1, \\ 0 & r/h > 1. \end{cases} \tag{2.30}$$

todo find whether this is the same for GIZMO. todo find how h is determined in GIZMO. The velocity of the macro-particle, on the other hand, is taken to be a delta function, such that the macro-particles have a single defined velocity.

When the patches represented by two macro-particles overlap, we can compute the interaction rate between them. The rate of scattering of a macro-particle j off a target particle i is given by

$$\Gamma(i|j) = (\sigma/m) m_p |\mathbf{v}_i - \mathbf{v}_j| g_{ji}, \tag{2.31}$$

where σ/m is the familiar cross-section to mass ratio and g_{ij} is a number density factor whose purpose is account for the overlap of the two macro-particles' smoothing kernels. It is given by

$$g_{ji} = \int_0^h d^3\mathbf{x}'\, W(|\mathbf{x}'|, h)\, W(|\delta\mathbf{x}_{ji} + \mathbf{x}'|, h), \tag{2.32}$$

with $\delta\mathbf{x}_{ji}$ the displacement vector between the macro-particle positions.

Over the course of a time step δt, the probability of an interaction of macro-particle j off target macro-particle i is given by

$$P(i|j) = \Gamma(i|j)\,\delta t. \tag{2.33}$$

The total probability of interaction between these two particles in this time step, then, would be the average of the two directed probabilities, i.e.

$$P_{ij} = \frac{1}{2}\left(P(i|j) + P(j|i)\right). \tag{2.34}$$

To actually represent the interaction, then, one draws a random number and adjusts the velocities of the particles if the number lies below the probability. The velocities are adjusted in a manner consistent with an elastic scattering which is isotropic in the center of mass frame.

More details are presented in [49], including the derivation of the scattering rate formula from the Boltzmann equation. We use the implementation which is packaged with the publicly-available GIZMO simulation suite.

Chapter 3

Sagittarius

3.1 Overview

Sagittarius (Sgr) is a dwarf spheroidal (dSph) galaxy in the Milky Way. It was the ninth dwarf satellite discovered in the Milky Way, and the last to be discovered before the advent of digital surveys [52]. It was identified in 1994 by Ibata et al. [22] as a dwarf satellite in the constellation of Sagittarius (hence its name). The authors then noted that it was the closest known galaxy to the Milky Way of any known at the time, and this has largely remained true to the present. One quirk about Sgr that was noted at the time was that it "is elongated towards the plane of the Milky Way, suggesting that it is undergoing some tidal disruption before being absorbed by the Milky Way." This would turn out to be a very important feature of Sgr to explain.

In the years since, many studies have been performed to try to understand and quantify various properties of Sgr, like its mass, orbital time, and the reason for its elongated shape. By 2000, it was believed that the elongation was the result of tidal shearing [23], meaning that accurately describing the orbital history of Sgr is essential. Further, this means we can expect that the stripping of stars by tidal forces may play a significant role in its evolution. Jiang and Binney [23] thus explored the parameter space for the initial mass and radius of Sgr, finding that a wide range of parameters are possible, from an initial mass of $\sim 10^{11}$ $M_\odot$ and Galactocentric distance of $\gtrsim 200$ kpc to mass $\sim 10^9$ $M_\odot$ and distance ~ 60 kpc.

Shortly thereafter, Majewski et al. used the Two Micron All Sky Survey (2MASS) to map Sgr, forming the first canonical model of Sgr [29]. Their characterization of Sgr included a description of a *stream* of stars that had been tidally stripped from Sagittarius, forming leading and trailing "tidal tails". These tails, they note, "lie along a well-defined orbital plane about the Galactic center." Moreover, they state that the lack of precession in the tidal debris is indicative

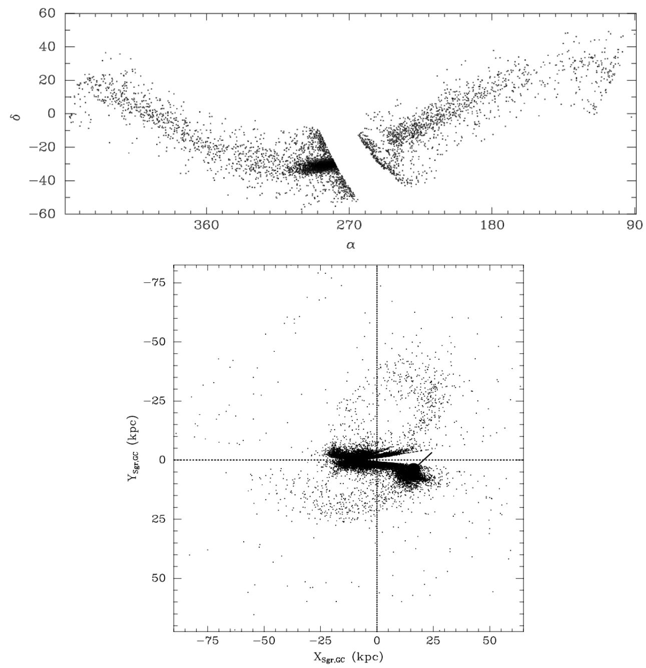

Figure 3.1: Sgr debris in (top) equatorial coordinates and (bottom) in the orbital plane with the Galactic center at the origin. Reproduced from Figure 11 of [29].

of a nearly spherical gravitational potential for the Milky Way, recognizing the usefulness of the Sagittarius stream as a potential measure of the gravitational potential.

We have included a reproduction of Figure 11 from [29], a plot of a sample of Sgr debris stars in equatorial coordinates and in the orbital plane. It can be seen in Figure 3.1. The core of Sgr lies at approximately $(+20, -10)$ in the orbital coordinates, with the northern arm leading above it and the southern arc leading to the left.

A similar work was performed by Belokurov et al. in 2006, using the Sloan Digital Sky Survey (SDSS) [3]. They found the tidal stream of Sgr to be “clearly visible”, and found the leading tidal arm to be especially clear. We include their Figure 2, which shows a panoramic view of the stream cutting together the 2MASS stars of Majewski et al. with the SDSS stars of Belokurov et al. This can be found in our Figure 3.2.

The picture of Sagittarius as tidally disrupted with debris forming a long streaming arc about the Milky Way would turn out to be well-supported by further observations and studies. In the ensuing years, more studies were performed to improve the model and more accurately quantify the properties of the galaxy. We note in particular the work of Kunder and Chaboyer [26] who estimated the

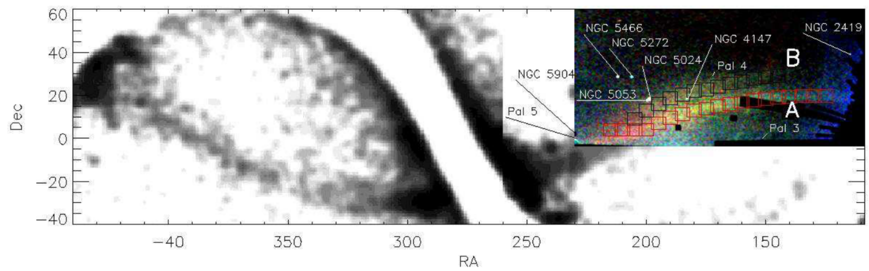

Figure 3.2: Sgr debris in equatorial coordinates, including both the 2MASS data from [29] (in grayscale) as well as SDSS data from [3] (in color). Reproduced from Figure 2 of [3].

distance to Sgr to be approximate 24.8 kpc.

todo add a discussion of stream coordinates?

3.2 Modern models

The next major discovery in the history of Sagittarius was the 2010 Law and Majewski model [27]. This model became the first two successfully satisfy the majority of existing constraints on the angular position, distance, and radial velocity of the tidal debris streams. It did so using a triaxial Milky Way halo; in other words, it dropped the typical assumption that the Milky Way halo is axisymmetric in the Galactic plane. One prediction of note from this model is that the current bound mass of Sgr is approximately 2.5×10^8 $M_\odot$. To obtain this, they use an initial mass of 6.4×10^8 $M_\odot$ with an infall orbit for around 8 Gyr in a fixed Galactic gravitational potential. It is worth noting that this initial mass lies in the régime where dynamical friction is small and the effects of tidal stripping on the Sgr progenitor are relatively small [12].

The resulting distribution of stars is shown in Figure 3.3. We reproduce their plots of the debris stream in terms of heliocentric coordinates and Galactocentric distances in the orbital plane. The coloring corresponds to the time at which the debris was stripped from Sgr. (Green is between the first and third apocenters, cyan between the third and fifth, magenta between the fifth and seventh, and orange later than the seventh.) Notice as well that they predict *two* wraps for both the leading ("L") and trailing ("T") stream arms.

Shortly thereafter came the model of Purcell et al. [45]. In their model, they explicitly account for the impact of the infall of Sagittarius on the evolution of the Milky Way disk, pointing out that all then-existing models of Sgr assume that its effects on the Galactic disk morphology are negligible. They found that Sgr created "significant perturbations to the outer disk" with noticeable effects on the evolution of the inner spirality. In their model, Sgr is represented

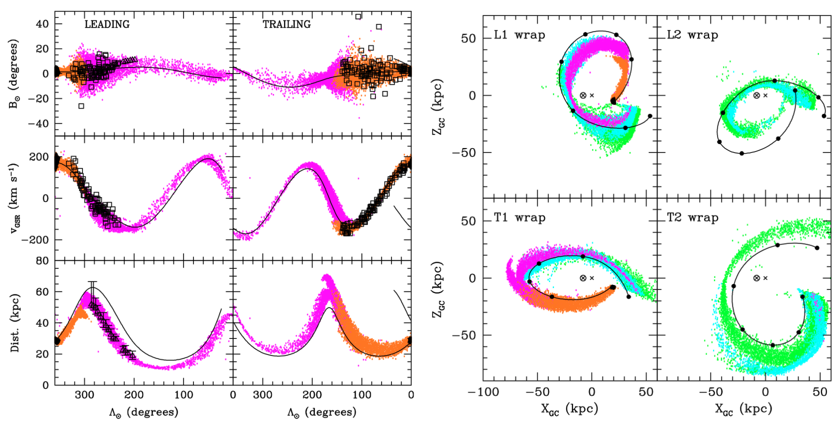

Figure 3.3: Sgr stellar debris streams according to the Law and Majewski 2010 model. On the left, debris stripped in the last $\sim$ 3 Gyr is shown in terms of stream and heliocentric coordinates. On the right, the first two wraps of the leading ("L") and trailing ("T") stream arms are shown in the orbital plane. These plots are reproduced from Figures 6 and 8 of [27].

as beginning with halo mass $10^{10.5}$ $M_\odot$ at a Galactocentric radius of 80 kpc in the Galactic plane. In order to account for tidal stripping that would have occurred between the infall of Sgr past the MW virial radius and the starting position they choose, they truncate the initial halo at the instantaneous Jacobi radius, $r_t = 23.2$ kpc. We note that such methods may produce qualitatively accurate representations of Sgr but are unlikely to accurately reflect the true orbital history of Sgr.

The resulting stream debris is shown in Figure 3.4. We show again both the stream in terms of heliocentric coordinates and in the orbital plane in terms of Galactocentric distances. We focus in particular on the "light Sgr" subplot of the Galactocentric figure. The figures show qualitatively similar patterns to the model of Law and Majewski [27], including the "L1" and "T1" wraps.

As such, the status until quite recently was that no existing Sagittarius model did could accurately account for a live Milky Way potential, the effects of dynamical friction, and the early infall of Sgr at Galactocentric radii of more than 60-80 kpc. In 2017, however, a new model which sought to solve all these problems was found by Dierickx and Loeb [12]. They simulate the infall of Sagittarius starting from its first crossing of the Milky Way virial radius approximately 8 Gyr ago using a live Milky Way gravitational potential and accounting for the full effects of dynamic friction. To find the best-fit model, they began by performing a parameter search with a fast and simple semi-analytic model. They then used these best-fit parameters in a full, high-resolution N-body simulation.

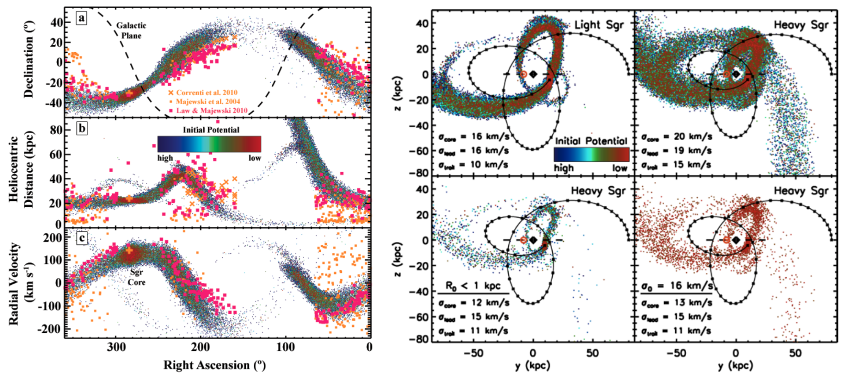

Figure 3.4: Sgr stellar debris streams according to the Purcell et al. 2011 model. On the left, debris is shown in terms of equatorial and heliocentric coordinates. On the right, the debris is shown in terms of Galactocentric distances in the orbital plane. We pay particular attention to the "light Sgr" subplot and note that the debris appears to contain approximately the same shape as the "L1" and "T1" wraps of the Law model. Figures reproduced from Figures 3 and S4 of [45].

The resulting simulation is able to reproduce both the leading and trailing stream arms to good agreement with both observed data and past models. Moreover, they note that the resulting model is the first to accurately reproduce existing data for debris observed 100 kpc away. The model also predicts the existence of an extension to the stream, including "the existence of several arms of the Sgr stream extending to hundreds of kiloparsecs." They note that this predicted structure matches the positions of the two most distant stars known in the Milky Way halo and serves as a testable prediction for data from future sky surveys.

This model is the one that we have (approximately) chosen to adopt for our simulations. The specific differences between our model and theirs will be elucidated in (todo add reference to simulation section). Dierickx and Loeb represent the Milky Way halo using a Hernquist distribution with total mass 1.25×10^{12} $M_\odot$ and scale radius 38.35 kpc. The Milky Way disk follows an exponential profile with mass 8.125×10^{10} $M_\odot$, scale length 3.5 kpc, and scale height 0.525 kpc. They also use a Hernquist bulge with mass 1.25×10^{10} $M_\odot$ and scale length 0.7 kpc. In their model, Sagittarius has a Hernquist halo with total mass 1.3×10^{10} $M_\odot$ and scale radius 9.81 kpc. It has an exponential disk with mass 6×10^8 $M_\odot$, scale length 0.85 kpc, and scale height 0.1275 kpc, and a Hernquist bulge with mass 5.2×10^8 $M_\odot$ and scale length 0.17 kpc.

As before, we include plots of the resulting stellar debris, both in terms of heliocentric coordinates and Galactocentric distances in the orbital plane. These plots are given in Figure 3.5. In this case, the familiar stream structure is

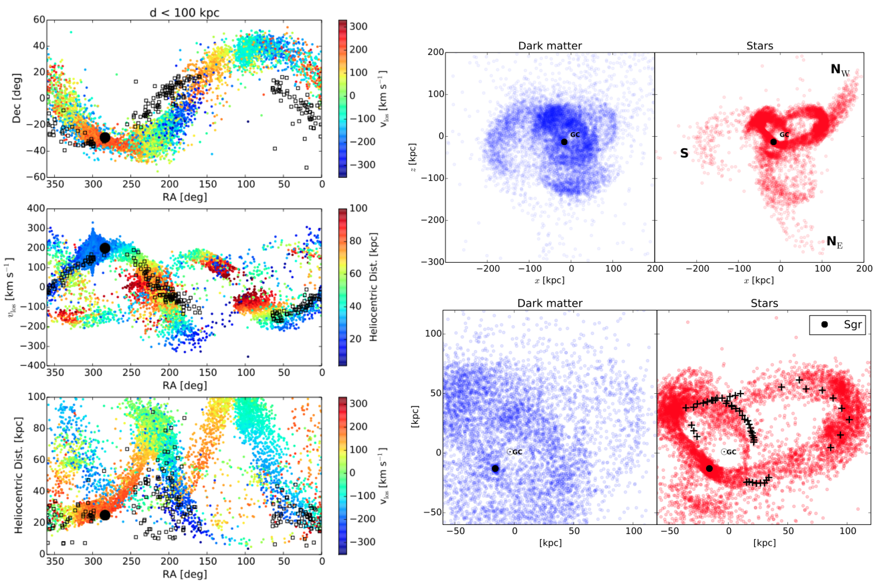

Figure 3.5: Sgr stellar debris according to the Dierickx and Loeb 2017 model. As before, we show the stream in equatorial and heliocentric coordinates on the left. On the right is the stream (and associated dark matter particles) in terms of Galactocentric distances in the orbital plane. The right top subfigure shows the full distributions, while the right bottom subfigure zooms into the more observationally relevant region. Comparisons to observed Sgr stars are also shown in black. Plots reproduced from Figure 8, 9, and 10 of [12].

once again reproduced, but with the inclusion of a significant extension to the stream arms far beyond the two wraps considered by Law and Majewski. The resulting distribution also appears to approximately reproduce the distributions of observed stars (observational data shown in black).

Chapter 4

Experimental setup

As stated previously, the core work of this thesis is performing N-body simulations of the infall of Sgr in the style of Dierickx et al. [12], varying the initial conditions and dark matter model to determine the resulting impacts on the evolution of the Sgr tidal debris stream. As such, we provide an overview of the setup of the simulations we performed in this section.

4.1 Pipeline and parameters

To begin our experimental pipeline, we first generate the initial distributions of stellar and dark matter particles using a package called GalactICS [11]. Each galaxy is modeled using a stellar disk and dark matter halo. The halo follows a Navarro-Frenk-White (NFW) profile

$$\rho_{\mathrm{halo}}(r) = \frac{M_{200}}{4\pi a^3 f(c)} \frac{1}{(r/a)(1+r/a)^2}, \tag{4.1}$$

where $f(c) = \log(1+c) - c/(1+c)$, M_{200} is the virial mass, a is the scale length, c is the concentration, and $c = r_{200}/a$. Here, we use a lowercase r to denote the radius in a spherical sense.

The stellar disk follows an exponential-sech^2 profile, given by

$$\rho_{\mathrm{disk}}(R, z) = \frac{M_{\mathrm{disk}}}{4\pi R_0^2 z_0} \exp(-R/R_0)\, \mathrm{sech}^2(z/z_0), \tag{4.2}$$

where R_0 is the disk scale length, z_0 is the disk scale height, and the capital R denotes the cylindrical radius in the plane of the disk.

Both of these distributions are subject to truncation beyond a certain radius, r_t, with truncation width dr_t. The truncation function comes from [60] and is

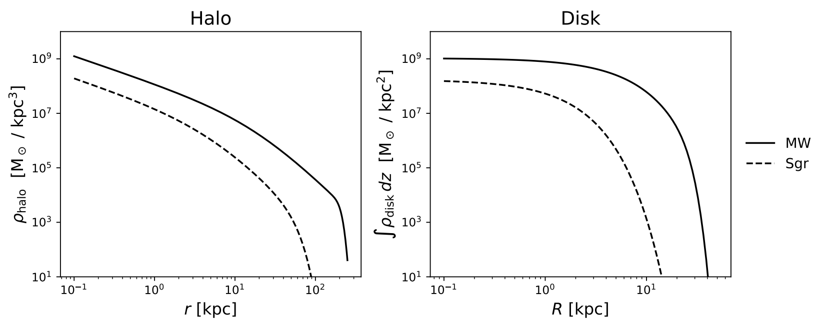

Figure 4.1: Initial profiles for the halo and disk of both galaxies. The halos follow a truncated NFW profile and the disks follow a truncated exponential-sech^2 profile. Note that the disk density is in cylindrical coordinates and is integrated over the z direction.

Parameters		MW	Sgr
Halo			
Virial mass	M_{200}	10^{12} M$_\odot$	10^{10} M$_\odot$
Virial radius	r_{200}	206 kpc	44 kpc
Concentration	c	10	8
Particles	$N_{\rm halo}$	1.16×10^6	1.17×10^4
Disk			
Mass	$M_{\rm disk}$	6.5×10^{10} M$_\odot$	6×10^8 M$_\odot$
Scale length	R_0	3.5 kpc	0.85 kpc
Scale height	z_0	0.53 kpc	0.13 kpc
Particles	$N_{\rm disk}$	2.03×10^6	1.17×10^4

Table 4.1: Parameters for the initial Milky Way and Sgr galaxies in our full simulation. These values are in large part taken from the work of [12].

given by

$$C(r; r_t, dr_t) = \frac{1}{2}\text{erfc}\left(\frac{r - r_t}{\sqrt{2}dr_t}\right). \tag{4.3}$$

For the halos, the truncation radius is simply the virial radius and the truncation width is 20 kpc. For the disks, the truncation radius is 25 kpc, the width is 5 kpc, and the truncation is only applied to R in the disk plane. The distributions, including the truncation parameter, can be seen in Figure 4.1.

Bundled with GalactICS is a subpackage called GadgetConverters, which provides a pipeline for converting the native output of GalactICS into a binary compatible with GADGET and derivative N-body simulation software. In this work, we use GIZMO [21], which is itself derived from GADGET-2 [54].

The parameters that were used for our simulations were largely taken from the

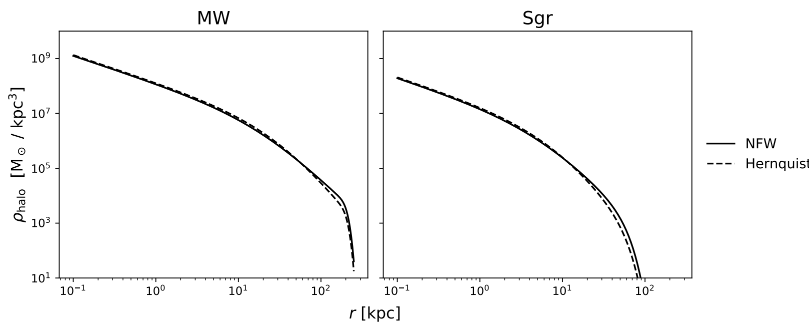

Figure 4.2: Comparison between the density profiles of the relevant truncated NFW and truncated Hernquist profiles for the Milky Way and Sgr galaxies in the Dierickx model. The NFW parameters can be found in Table 4.1. The Hernquist parameters are as follows: total MW halo mass 1.25×10^{12} $M_\odot$, MW scale radius 38.35 kpc, total Sgr halo mass 1.3×10^{10} $M_\odot$, Sgr scale radius 9.81 kpc.

work of Dierickx et al. [12]. They are summarized in Table 4.1. There are a few key differences between their model and our simulations, however. First, they used Hernquist profiles for their halos, while we use NFW distributions. The NFW parameters we use, however, come from their work, where they are given as the parameters which yield an approximately equivalent distribution. A comparison between their Hernquist and our NFW profiles is shown in Figure 4.2; the differences are quite small.

The second source of discrepancy between their work and ours is that we have less resolution in our stellar profile than in their work. This is in part because they used a Hernquist bulge in both their Milky Way and Sgr, wherer this has been omitted from our work. It is also because they used more stellar particles for the Sgr disk than we did (1.94×10^4 versus 1.17×10^4), owing to a technical error in our initial conditions creation pipeline.

The experiments performed herein were performed using GIZMO version (todo find out) on Princeton Research Computing's Della cluster. This cluster is an Intel cluster with $\geq$ 20 cores per node and $\geq$ 128 GB memory per node [44]. Our simulations often used around 10 GB of RAM and typically split the computation over 25 cores.

4.2 Equilibration

After generating the initial particle distributions for each galaxy, we evolved each one forward in time for a several Gyr to allow it to equilibrate. For our runs involving SIDM, we perform this equilibration run with SIDM microphysics turned on, allowing for the creation of a core in the central region of the dark

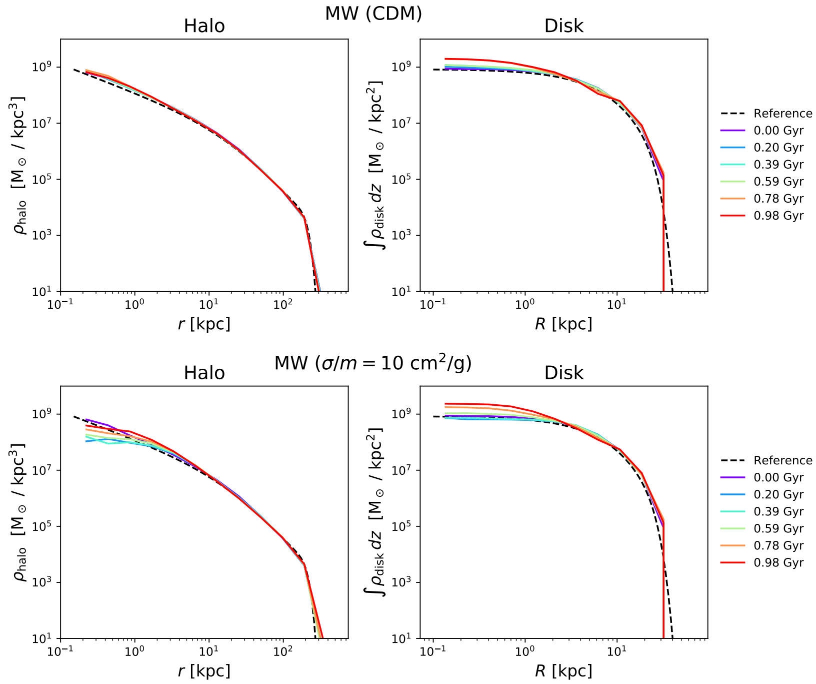

Figure 4.3: Evolution of the MW halo (left) and disk (right) during CDM (top) and SIDM (bottom) equilibration runs. The dashed line on the halo plots is the reference NFW distribution; on the disk plots it is the reference exponential-sech^2 distribution.

matter halo.

For each galaxy, we begin with the parameters discussed in the previous section and perform two equilibration runs: one using CDM microphysics and one using SIDM microphysics with a cross section of $\sigma/m = 10$ cm^2/g. In this study, we choose to use a somewhat high cross section in order to exaggerate any differences that may appear because of the presence of self-interaction. We note that future studies should consider a range of cross sections.

For the Milky Way equilibrations—both CDM and SIDM—we only evolve the galaxy forward for 1 Gyr, writing time stamps approximately every 0.1 Gyr. This is because we expect the initial distribution to be relatively close to equilibrium, especially when considering such a large galaxy. The resulting evolution of the mass density profiles are shown in Figure 4.3.

In these plots, we can see that the CDM halo starts in a state which is already close to equilibrium. The halo changes very little, and the disk slowly pulls a small amount of density in toward the center. The SIDM halo, however, almost immedately develops a rather substantial core, which slowly dissolves somewhat,

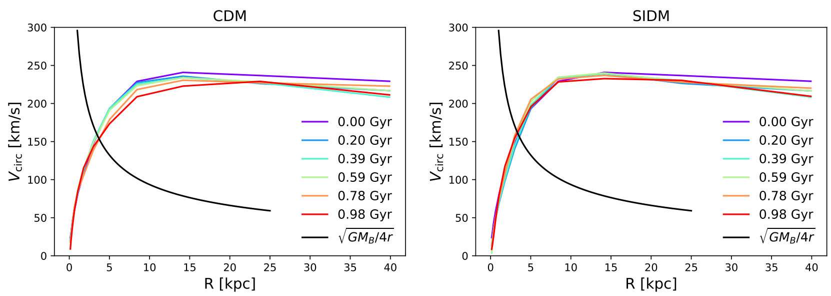

Figure 4.4: Evolution of rotation curves over time for the Milky Way disk in both the CDM and SIDM microphysics runs. Also plotted in black is $\sqrt{GM_b/4r}$, the circular velocity at the scale radius which would be expected if the disk mass followed a Hernquist profile.

leaving a small core with size $\sim$ 1 kpc. This is almost certainly because of the disk. As the disk equilibrates, its central density increases, increasing the gravitational potential in the center of the galaxy and counteracting the coring effect of self-interactions.

We can also compare these results to those we might have expected following the analytic formalism for determining the core size in Section 2.3. To begin, we need to find the scale radius r_0 and the center value of the gravitational potential $\Phi_B(0)$ in the "spherical disk" approximation. We can do so by using the following two relations:

$$\Phi_B(0) = -\frac{GM_B}{r_0} \tag{4.4}$$

$$V_B(r_0) = \frac{\sqrt{-\Phi_B(0)}}{2}, \tag{4.5}$$

where M_B is the mass of the baryons in the disk and V_B is the circular velocity of baryons at the given radius. Together, these imply that $V_B(r_0) = \sqrt{GM_B/4r_0}$. After truncation, our disk has a total mass of $M_B = 8.1 \times 10^{10}$ M$_\odot$. Thus, we can plot the rotation curve of our disk and look for its intersection with $\sqrt{GM_B/4r_0}$. This should give us the values of r_0 and $V_B(r_0)$. The rotation curves for both the CDM and SIDM curves are plotted in Figure 4.4. They show $r_0 \approx 3.5$ kpc with a corresponding circular velocity $V_B(r_0) \approx 160$ km/s.

Looking back at Figure 4.3, we can estimate the central density of the halo to be $\rho_0 \approx 10^9$ M$_\odot$/kpc^3. Using a velocity of dispersion of approximately 150 km/s (as suggested for the Milky Way in [24]), we can thus find $a_0 = 29.43$ and $a_1 = 4.44$. Plugging these in to Equation 2.28, we obtain an estimate for the core size of 0.55 kpc. This is approximately consistent with the small core seen in the final distribution attained in the SIDM equilibration.

For the Sgr equilibrations, however, we evolved the galaxy much farther forward

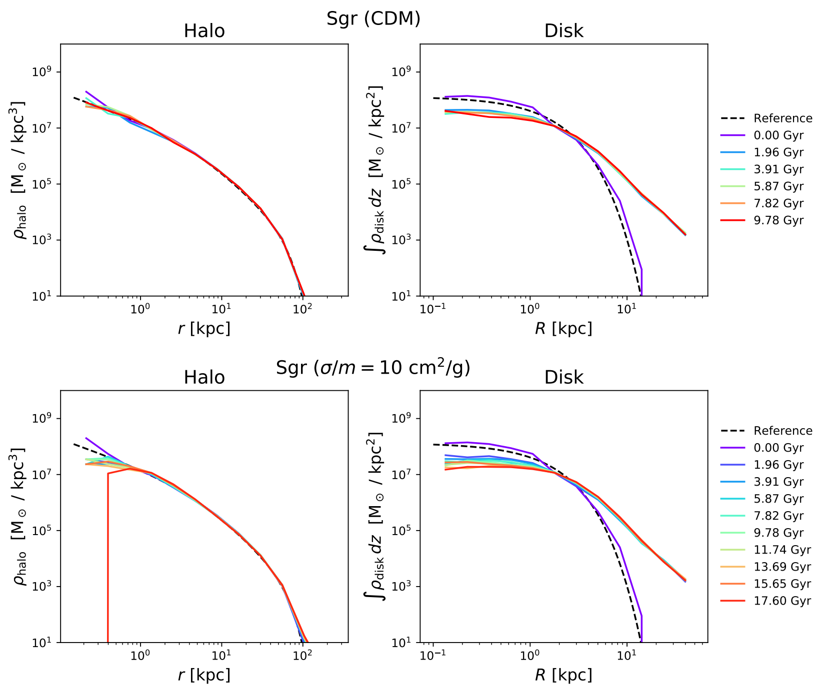

Figure 4.5: Evolution of the Sgr halo (left) and disk (right) during CDM (top) and SIDM (bottom) equilibration runs. The dashed line on the halo plots is the reference NFW distribution; on the disk plots it is the reference exponential-sech^2 distribution. We note in particular that the SIDM run results in generally depressed densities for both the halo and disk at low radii.

in time: approximately 10 Gyr for the CDM case and 20 Gyr for SIDM. These evolution times do not correspond to a physical orbit (especially given that the SIDM case would exceed the lifetime of the Universe). Rather, the initial Sgr disk distribution was found to be a bit unstable. We also wanted to be absolutely certain that the SIDM case would develop a cored profile. The evolution of the resulting Sgr mass profiles is shown in Figure 4.5.

In these plots, we see that the initial exponential-sech^2 distribution for the disk was not very close to equilibrium. Almost immediately, the disk redistributes itself more outwardly, with more of its mass at larger radii and a falling inner density. In the case of CDM physics, this happens within the first two Gyr, and the distribution holds relatively constant from there on. In the SIDM case, however, the distribution appears to continue falling somewhat, attaining central density values around half those of the CDM disk.

In the case of the halo, we notice that the distribution holds relatively constant in the CDM case and agrees well with the reference NFW distribution. In the

SIDM case, however, we see the slow development of a small core at low radii. This core appears to have a size of ≈ 1 kpc.

We can again apply the analytic expressions derived before to obtain an estimate for the expected core size. In this case, we note that the Sgr galaxy is well-approximated by the dark matter-dominated limit, so we will use the corresponding limit of the approximate core size. We again take $r_0 = 3.5$ kpc, and we estimate $\rho_0 \approx 10^{7.5}$ $\mathrm{M}_\odot/\mathrm{kpc}^3$ from Figure 4.5. We also estimate the central velocity dispersion to be $\sigma_0 \approx 21$ km/s, following the results reported in [23]. Using Equation 2.27, we obtain an estimated core size of ≈ 1 kpc. We find this to roughly correspond to the core seen in the final time stamp of the evolved mass density profile.

With the equilibrated MW and Sgr galaxies in both the cuspy and cored régimes, we combine them to give us two initial conditions for mergers: cuspy and cored. The Milky Way is left at its position from the equilibration run, as its center of mass will be close to the origin and its net velocity will be close to zero. Sgr is placed such that its center of mass lies at the point $[125, 0, 0]$ and is given an initial velocity $[-10, 0, 70]$. These values correspond to the best fit values found in [12].

Bibliography

[1] Heinz Andernach and Fritz Zwicky. "English and Spanish Translation of Zwicky's (1933) The Redshift of Extragalactic Nebulae". In: *arXiv:1711.01693 [astro-ph]* (Nov. 2017). arXiv: 1711.01693. URL: http://arxiv.org/abs/1711.01693 (visited on 04/19/2021).

[2] Horace W. Babcock. "The rotation of the Andromeda Nebula". In: *Lick Observatory Bulletin* 19 (1939), pp. 41–51. ISSN: 0075-9317. DOI: 10.5479/ADS/bib/1939LicOB.19.41B. URL: http://adsabs.harvard.edu/abs/1939LicOB..19...41B (visited on 04/19/2021).

[3] V. Belokurov et al. "The Field of Streams: Sagittarius and Its Siblings". In: *The Astrophysical Journal Letters* 642 (May 2006), pp. L137–L140. ISSN: 0004-637X. DOI: 10.1086/504797. URL: http://adsabs.harvard.edu/abs/2006ApJ...642L.137B (visited on 04/24/2021).

[4] Lars Bergström and Ariel Goobar. *Cosmology and particle astrophysics*. en. 2. ed., reprinted. Springer Praxis books in astronomy and planetary science. OCLC: 254584818. Berlin: Springer, 2008. ISBN: 978-3-540-32924-4.

[5] James Binney and Scott Tremaine. *Galactic dynamics*. 2nd ed. Princeton series in astrophysics. Princeton: Princeton University Press, 2008. ISBN: 978-0-691-13026-2 978-0-691-13027-9.

[6] James S. Bullock and Michael Boylan-Kolchin. "Small-Scale Challenges to the ΛCDM Paradigm". In: *Annual Review of Astronomy and Astrophysics* 55 (Aug. 2017), pp. 343–387. ISSN: 0066-4146. DOI: 10.1146/annurev-astro-091916-055313. URL: http://adsabs.harvard.edu/abs/2017ARA%26A..55..343B (visited on 04/22/2021).

[7] Andreas Burkert. "The Structure and Evolution of Weakly Self-interacting Cold Dark Matter Halos". In: *The Astrophysical Journal Letters* 534 (May 2000), pp. L143–L146. ISSN: 0004-637X. DOI: 10.1086/312674. URL: http://adsabs.harvard.edu/abs/2000ApJ...534L.143B (visited on 04/23/2021).

[8] T. K. Chan et al. "The impact of baryonic physics on the structure of dark matter haloes: the view from the FIRE cosmological simulations". In: *Monthly Notices of the Royal Astronomical Society* 454 (Dec. 2015), pp. 2981–3001. ISSN: 0035-8711. DOI: 10.1093/mnras/stv2165. URL:

http://adsabs.harvard.edu/abs/2015MNRAS.454.2981C (visited on 04/22/2021).

[9] James M. Cline et al. “Composite strongly interacting dark matter”. In: *Phys. Rev. D* 90.1 (July 2014). arXiv: 1312.3325, p. 015023. ISSN: 1550-7998, 1550-2368. DOI: 10.1103/PhysRevD.90.015023. URL: http://arxiv.org/abs/1312.3325 (visited on 01/05/2021).

[10] Romeel Davé et al. “Halo Properties in Cosmological Simulations of Self-interacting Cold Dark Matter”. In: *The Astrophysical Journal* 547 (Feb. 2001), pp. 574–589. ISSN: 0004-637X. DOI: 10.1086/318417. URL: http://adsabs.harvard.edu/abs/2001ApJ...547..574D (visited on 04/23/2021).

[11] N. Deg et al. “GalactICS with Gas”. In: *Monthly Notices of the Royal Astronomical Society* 486.4 (July 2019). arXiv: 1904.12700, pp. 5391–5399. ISSN: 0035-8711, 1365-2966. DOI: 10.1093/mnras/stz1203. URL: http://arxiv.org/abs/1904.12700 (visited on 01/05/2021).

[12] Marion Dierickx and Abraham Loeb. “Predicted Extension of the Sagittarius Stream to the Milky Way Virial Radius”. In: *ApJ* 836.1 (Feb. 2017). arXiv: 1611.00089, p. 92. ISSN: 1538-4357. DOI: 10.3847/1538-4357/836/1/92. URL: http://arxiv.org/abs/1611.00089 (visited on 09/13/2020).

[13] Scott Dodelson and Fabian Schmidt. *Modern Cosmology*. en. 2nd ed. Elsevier, 2021. ISBN: 978-0-12-815948-4. DOI: 10.1016/B978-0-12-815948-4.00002-4. URL: https://linkinghub.elsevier.com/retrieve/pii/B9780128159484000024 (visited on 03/23/2021).

[14] John Dubinski and R. G. Carlberg. “The structure of cold dark matter halos”. In: *The Astrophysical Journal* 378 (Sept. 1991), pp. 496–503. ISSN: 0004-637X. DOI: 10.1086/170451. URL: http://adsabs.harvard.edu/abs/1991ApJ...378..496D (visited on 04/19/2021).

[15] Jaan Einasto et al. “Missing mass around galaxies: morphological evidence”. en. In: *Nature* 252.5479 (Nov. 1974). Number: 5479 Publisher: Nature Publishing Group, pp. 111–113. ISSN: 1476-4687. DOI: 10.1038/252111a0. URL: https://www.nature.com/articles/252111a0 (visited on 04/19/2021).

[16] Oliver D. Elbert et al. “Core formation in dwarf haloes with self-interacting dark matter: no fine-tuning necessary”. In: *Monthly Notices of the Royal Astronomical Society* 453 (Oct. 2015), pp. 29–37. ISSN: 0035-8711. DOI: 10.1093/mnras/stv1470. URL: http://adsabs.harvard.edu/abs/2015MNRAS.453...29E (visited on 04/23/2021).

[17] Ricardo Flores et al. “Rotation curves from baryonic infall - Dependence on disk-to-halo ratio, initial angular momentum, and core radius, and comparison with data”. In: *The Astrophysical Journal* 412 (Aug. 1993), pp. 443–454. ISSN: 0004-637X. DOI: 10.1086/172934. URL: http://adsabs.harvard.edu/abs/1993ApJ...412..443F (visited on 04/19/2021).

[18] Carlos S. Frenk et al. “The formation of dark halos in a universe dominated by cold dark matter”. In: *The Astrophysical Journal* 327 (Apr. 1988), pp. 507–525. ISSN: 0004-637X. DOI: 10.1086/166213. URL: http://adsabs.harvard.edu/abs/1988ApJ...327..507F (visited on 04/19/2021).

[19] Lars Hernquist. “An analytical model for spherical galaxies and bulges”. In: *The Astrophysical Journal* 356 (June 1990), pp. 359–364. ISSN: 0004-637X. DOI: 10.1086/168845. URL: http://adsabs.harvard.edu/abs/1990ApJ...356..359H (visited on 04/19/2021).

[20] Erik Holmberg. “On the masses of double galaxies”. In: *Meddelanden fran Lunds Astronomiska Observatorium Serie I* 186 (June 1954), pp. 1–20. URL: http://adsabs.harvard.edu/abs/1954MeLuF.186....1H (visited on 04/19/2021).

[21] Philip F. Hopkins. “A new class of accurate, mesh-free hydrodynamic simulation methods”. In: *Monthly Notices of the Royal Astronomical Society* 450 (June 2015), pp. 53–110. ISSN: 0035-8711. DOI: 10.1093/mnras/stv195. URL: http://adsabs.harvard.edu/abs/2015MNRAS.450...53H (visited on 04/23/2021).

[22] R. A. Ibata, G. Gilmore, and M. J. Irwin. “A dwarf satellite galaxy in Sagittarius”. en. In: *Nature* 370.6486 (July 1994). Number: 6486 Publisher: Nature Publishing Group, pp. 194–196. ISSN: 1476-4687. DOI: 10.1038/370194a0. URL: https://www.nature.com/articles/370194a0 (visited on 04/23/2021).

[23] Ing-Guey Jiang and James Binney. “The orbit and mass of the Sagittarius dwarf galaxy”. In: *Monthly Notices of the Royal Astronomical Society* 314 (May 2000), pp. 468–474. ISSN: 0035-8711. DOI: 10.1046/j.1365-8711.2000.03311.x. URL: http://adsabs.harvard.edu/abs/2000MNRAS.314..468J (visited on 04/23/2021).

[24] Manoj Kaplinghat et al. “Tying Dark Matter to Baryons with Self-Interactions”. In: *Physical Review Letters* 113 (July 2014), p. 021302. ISSN: 0031-9007. DOI: 10.1103/PhysRevLett.113.021302. URL: http://adsabs.harvard.edu/abs/2014PhRvL.113b1302K (visited on 04/23/2021).

[25] Graham D. Kribs and Ethan T. Neil. “Review of strongly-coupled composite dark matter models and lattice simulations”. In: *Int. J. Mod. Phys. A* 31.22 (Aug. 2016). arXiv: 1604.04627, p. 1643004. ISSN: 0217-751X, 1793-656X. DOI: 10.1142/S0217751X16430041. URL: http://arxiv.org/abs/1604.04627 (visited on 01/05/2021).

[26] Andrea Kunder and Brian Chaboyer. “Distance to the Sagittarius Dwarf Galaxy Using Macho Project RR Lyrae Stars”. In: *The Astronomical Journal* 137 (May 2009), pp. 4478–4486. ISSN: 0004-6256. DOI: 10.1088/0004-6256/137/5/4478. URL: http://adsabs.harvard.edu/abs/2009AJ....137.4478K (visited on 04/23/2021).

[27] David R. Law and Steven R. Majewski. “The Sagittarius Dwarf Galaxy: A Model for Evolution in a Triaxial Milky Way Halo”. In: *The Astrophysical Journal* 714 (May 2010), pp. 229–254. ISSN: 0004-637X. DOI: 10.1088/0004-637X/714/1/229. URL: http://adsabs.harvard.edu/abs/2010ApJ...714..229L (visited on 04/23/2021).

[28] W. Lohmann. “Die Masse der Galaxis”. de. In: *Z. Physik* 144.1-3 (Feb. 1956), pp. 66–75. ISSN: 1434-6001, 1434-601X. DOI: 10.1007/BF01327068. URL: http://link.springer.com/10.1007/BF01327068 (visited on 04/19/2021).

[29] Steven R. Majewski et al. "A Two Micron All Sky Survey View of the Sagittarius Dwarf Galaxy. I. Morphology of the Sagittarius Core and Tidal Arms". In: *The Astrophysical Journal* 599 (Dec. 2003), pp. 1082–1115. ISSN: 0004-637X. DOI: 10.1086/379504. URL: http://adsabs.harvard.edu/abs/2003ApJ...599.1082M (visited on 04/23/2021).

[30] Massimo Meneghetti et al. "Giant cluster arcs as a constraint on the scattering cross-section of dark matter". In: *Monthly Notices of the Royal Astronomical Society* 325 (July 2001), pp. 435–442. ISSN: 0035-8711. DOI: 10.1046/j.1365-8711.2001.04477.x. URL: http://adsabs.harvard.edu/abs/2001MNRAS.325..435M (visited on 04/23/2021).

[31] Jordi Miralda-Escudé. "A Test of the Collisional Dark Matter Hypothesis from Cluster Lensing". In: *The Astrophysical Journal* 564 (Jan. 2002), pp. 60–64. ISSN: 0004-637X. DOI: 10.1086/324138. URL: http://adsabs.harvard.edu/abs/2002ApJ...564...60M (visited on 04/23/2021).

[32] Subhendra Mohanty. *Astroparticle Physics and Cosmology: Perspectives in the Multimessenger Era.* en. Vol. 975. Lecture Notes in Physics. Cham: Springer International Publishing, 2020. ISBN: 978-3-030-56200-7 978-3-030-56201-4. DOI: 10.1007/978-3-030-56201-4. URL: http://link.springer.com/10.1007/978-3-030-56201-4 (visited on 03/22/2021).

[33] Ben Moore et al. "Collisional versus Collisionless Dark Matter". In: *The Astrophysical Journal Letters* 535 (May 2000), pp. L21–L24. ISSN: 0004-637X. DOI: 10.1086/312692. URL: http://adsabs.harvard.edu/abs/2000ApJ...535L..21M (visited on 04/23/2021).

[34] Julio F. Navarro, Carlos S. Frenk, and Simon D. M. White. "A Universal Density Profile from Hierarchical Clustering". In: *arXiv:astro-ph/9611107* (Oct. 1997). arXiv: astro-ph/9611107. DOI: 10.1086/304888. URL: http://arxiv.org/abs/astro-ph/9611107 (visited on 04/19/2021).

[35] Julio F. Navarro, Carlos S. Frenk, and Simon D. M. White. "The Structure of Cold Dark Matter Halos". In: *arXiv:astro-ph/9508025* (Aug. 1995). arXiv: astro-ph/9508025. DOI: 10.1086/177173. URL: http://arxiv.org/abs/astro-ph/9508025 (visited on 04/19/2021).

[36] J. H. Oort. "Some Problems Concerning the Structure and Dynamics of the Galactic System and the Elliptical Nebulae NGC 3115 and 4494." en. In: *ApJ* 91 (Apr. 1940), p. 273. ISSN: 0004-637X, 1538-4357. DOI: 10.1086/144167. URL: http://adsabs.harvard.edu/doi/10.1086/144167 (visited on 04/19/2021).

[37] J. H. Oort. "The force exerted by the stellar system in the direction perpendicular to the galactic plane and some related problems". In: *Bulletin of the Astronomical Institutes of the Netherlands* 6 (Aug. 1932), p. 249. ISSN: 0365-8910. URL: http://adsabs.harvard.edu/abs/1932BAN.....6..249O (visited on 04/19/2021).

[38] J. P. Ostriker and P. J. E. Peebles. "A Numerical Study of the Stability of Flattened Galaxies: or, can Cold Galaxies Survive?" In: *The Astrophysical Journal* 186 (Dec. 1973), pp. 467–480. ISSN: 0004-637X. DOI: 10.1086/152513. URL: http://adsabs.harvard.edu/abs/1973ApJ...186..467O (visited on 04/19/2021).

[39] J. P. Ostriker, P. J. E. Peebles, and A. Yahil. “The size and mass of galaxies, and the mass of the universe”. In: *The Astrophysical Journal Letters* 193 (Oct. 1974), pp. L1–L4. ISSN: 0004-637X. DOI: 10.1086/181617. URL: http://adsabs.harvard.edu/abs/1974ApJ...193L...1O (visited on 04/19/2021).

[40] Thornton Page. “Average Masses and Mass-Luminosity Ratios of the Double Galaxies.” In: *The Astrophysical Journal* 132 (Nov. 1960), pp. 910–912. ISSN: 0004-637X. DOI: 10.1086/146995. URL: http://adsabs.harvard.edu/abs/1960ApJ...132..910P (visited on 04/19/2021).

[41] S. Perlmutter et al. “Measurements of Ω and Λ from 42 High-Redshift Supernovae”. In: *The Astrophysical Journal* 517 (June 1999), pp. 565–586. ISSN: 0004-637X. DOI: 10.1086/307221. URL: http://adsabs.harvard.edu/abs/1999ApJ...517..565P (visited on 04/22/2021).

[42] Annika H. G. Peter et al. “Cosmological simulations with self-interacting dark matter - II. Halo shapes versus observations”. In: *Monthly Notices of the Royal Astronomical Society* 430 (Mar. 2013), pp. 105–120. ISSN: 0035-8711. DOI: 10.1093/mnras/sts535. URL: http://adsabs.harvard.edu/abs/2013MNRAS.430..105P (visited on 04/23/2021).

[43] Andrew Pontzen and Fabio Governato. “How supernova feedback turns dark matter cusps into cores”. In: *Monthly Notices of the Royal Astronomical Society* 421 (Apr. 2012), pp. 3464–3471. ISSN: 0035-8711. DOI: 10.1111/j.1365-2966.2012.20571.x. URL: http://adsabs.harvard.edu/abs/2012MNRAS.421.3464P (visited on 04/22/2021).

[44] Princeton Research Computing. *Della*. en. URL: https://researchcomputing.princeton.edu/systems/della (visited on 04/25/2021).

[45] Chris W. Purcell et al. “The Sagittarius impact as an architect of spirality and outer rings in the Milky Way”. In: *Nature* 477 (Sept. 2011), pp. 301–303. ISSN: 0028-0836. DOI: 10.1038/nature10417. URL: http://adsabs.harvard.edu/abs/2011Natur.477..301P (visited on 04/23/2021).

[46] Adam G. Riess et al. “Observational Evidence from Supernovae for an Accelerating Universe and a Cosmological Constant”. In: *The Astronomical Journal* 116 (Sept. 1998), pp. 1009–1038. ISSN: 0004-6256. DOI: 10.1086/300499. URL: http://adsabs.harvard.edu/abs/1998AJ....116.1009R (visited on 04/22/2021).

[47] M. S. Roberts and A. H. Rots. “Comparison of Rotation Curves of Different Galaxy Types”. In: *Astronomy and Astrophysics* 26 (Aug. 1973), pp. 483–485. ISSN: 0004-6361. URL: http://adsabs.harvard.edu/abs/1973A%26A....26..483R (visited on 04/19/2021).

[48] M. S. Roberts and R. N. Whitehurst. “The rotation curve and geometry of M31 at large galactocentric distances.” In: *The Astrophysical Journal* 201 (Oct. 1975), pp. 327–346. ISSN: 0004-637X. DOI: 10.1086/153889. URL: http://adsabs.harvard.edu/abs/1975ApJ...201..327R (visited on 04/19/2021).

[49] Miguel Rocha et al. “Cosmological simulations with self-interacting dark matter - I. Constant-density cores and substructure”. In: *Monthly Notices of the Royal Astronomical Society* 430 (Mar. 2013), pp. 81–104. ISSN: 0035-

8711. DOI: 10.1093/mnras/sts514. URL: http://adsabs.harvard.edu/abs/2013MNRAS.430...81R (visited on 04/23/2021).

[50] Vera C. Rubin and W. Kent Ford Jr. “Rotation of the Andromeda Nebula from a Spectroscopic Survey of Emission Regions”. In: *The Astrophysical Journal* 159 (Feb. 1970), p. 379. ISSN: 0004-637X. DOI: 10.1086/150317. URL: http://adsabs.harvard.edu/abs/1970ApJ...159..379R (visited on 04/19/2021).

[51] Peter Schneider. *Extragalactic Astronomy and Cosmology*. en. Berlin, Heidelberg: Springer Berlin Heidelberg, 2015. ISBN: 978-3-642-54082-0 978-3-642-54083-7. DOI: 10.1007/978-3-642-54083-7. URL: http://link.springer.com/10.1007/978-3-642-54083-7 (visited on 03/22/2021).

[52] Joshua D. Simon. “The Faintest Dwarf Galaxies”. In: *Annual Review of Astronomy and Astrophysics* 57 (Aug. 2019), pp. 375–415. ISSN: 0066-4146. DOI: 10.1146/annurev-astro-091918-104453. URL: http://adsabs.harvard.edu/abs/2019ARA%26A..57..375S (visited on 04/22/2021).

[53] David N. Spergel and Paul J. Steinhardt. “Observational Evidence for Self-Interacting Cold Dark Matter”. In: *Physical Review Letters* 84 (Apr. 2000), pp. 3760–3763. ISSN: 0031-9007. DOI: 10.1103/PhysRevLett.84.3760. URL: http://adsabs.harvard.edu/abs/2000PhRvL..84.3760S (visited on 04/22/2021).

[54] Volker Springel. “The cosmological simulation code GADGET-2”. In: *Monthly Notices of the Royal Astronomical Society* 364.4 (Dec. 2005). arXiv: astro-ph/0505010, pp. 1105–1134. ISSN: 0035-8711, 1365-2966. DOI: 10.1111/j.1365-2966.2005.09655.x. URL: http://arxiv.org/abs/astro-ph/0505010 (visited on 01/05/2021).

[55] Virginia Trimble. “Existence and Nature of Dark Matter in the Universe”. en. In: *Annu. Rev. Astron. Astrophys.* 25.1 (Sept. 1987), pp. 425–472. ISSN: 0066-4146, 1545-4282. DOI: 10.1146/annurev.aa.25.090187.002233. URL: http://www.annualreviews.org/doi/10.1146/annurev.aa.25.090187.002233 (visited on 03/22/2021).

[56] Virginia Trimble. “History of Dark Matter in Galaxies”. In: *Planets, Stars, and Stellar Systems: Galactic Structure and Stellar Populations*. Ed. by Terry D. Oswalt and Gerard Gilmore. Vol. 5. Dordrecht: Springer Netherlands, 2013, pp. 1091–1118.

[57] Sean Tulin and Hai-Bo Yu. “Dark matter self-interactions and small scale structure”. In: *Physics Reports* 730 (Feb. 2018), pp. 1–57. ISSN: 0370-1573. DOI: 10.1016/j.physrep.2017.11.004. URL: http://adsabs.harvard.edu/abs/2018PhR...730....1T (visited on 04/19/2021).

[58] Sean Tulin, Hai-Bo Yu, and Kathryn M. Zurek. “Beyond Collisionless Dark Matter: Particle Physics Dynamics for Dark Matter Halo Structure”. In: *Phys. Rev. D* 87.11 (June 2013). arXiv: 1302.3898, p. 115007. ISSN: 1550-7998, 1550-2368. DOI: 10.1103/PhysRevD.87.115007. URL: http://arxiv.org/abs/1302.3898 (visited on 01/05/2021).

[59] Sean Tulin, Hai-Bo Yu, and Kathryn M. Zurek. “Resonant Dark Forces and Small Scale Structure”. In: *Phys. Rev. Lett.* 110.11 (Mar. 2013). arXiv: 1210.0900, p. 111301. ISSN: 0031-9007, 1079-7114. DOI: 10.1103/

PhysRevLett.110.111301. URL: http://arxiv.org/abs/1210.0900 (visited on 01/05/2021).

[60] Lawrence M. Widrow, Brent Pym, and John Dubinski. "Dynamical Blueprints for Galaxies". In: *ApJ* 679.2 (June 2008). arXiv: 0801.3414, pp. 1239–1259. ISSN: 0004-637X, 1538-4357. DOI: 10.1086/587636. URL: http://arxiv.org/abs/0801.3414 (visited on 01/07/2021).

[61] Naoki Yoshida et al. "Collisional Dark Matter and the Structure of Dark Halos". In: *The Astrophysical Journal Letters* 535 (June 2000), pp. L103–L106. ISSN: 0004-637X. DOI: 10.1086/312707. URL: http://adsabs.harvard.edu/abs/2000ApJ...535L.103Y (visited on 04/23/2021).

[62] Naoki Yoshida et al. "Weakly Self-interacting Dark Matter and the Structure of Dark Halos". In: *The Astrophysical Journal Letters* 544 (Dec. 2000), pp. L87–L90. ISSN: 0004-637X. DOI: 10.1086/317306. URL: http://adsabs.harvard.edu/abs/2000ApJ...544L..87Y (visited on 04/23/2021).

[63] Jesús Zavala, Mark Vogelsberger, and Matthew G. Walker. "Constraining self-interacting dark matter with the Milky Way's dwarf spheroidals". In: *Monthly Notices of the Royal Astronomical Society* 431 (Apr. 2013), pp. L20–L24. ISSN: 0035-8711. DOI: 10.1093/mnrasl/sls053. URL: http://adsabs.harvard.edu/abs/2013MNRAS.431L..20Z (visited on 04/23/2021).

[64] F. Zwicky. "Die Rotverschiebung von extragalaktischen Nebeln". In: *Helvetica Physica Acta* 6 (1933), pp. 110–127. ISSN: 0018-0238. URL: http://adsabs.harvard.edu/abs/1933AcHPh...6..110Z (visited on 04/19/2021).